JPIS
Journal of Periodontal & Implant Science

Research Article

Check for updates

Comparisons of the diagnostic accuracies of optical coherence tomography, micro-computed tomography, and histology in periodontal disease: an *ex vivo* study

Jin-Young Park[1], Jung-Ho Chung[2], Jung-Seok Lee[1], Hee-Jin Kim[3], Seong-Ho Choi[1], Ui-Won Jung[1,*]

[1]Department of Periodontology, Research Institute for Periodontal Regeneration, Yonsei University College of Dentistry, Seoul, Korea
[2]Intelligence R&D Laboratory, LG Electronics, Seoul, Korea
[3]Division of Anatomy and Developmental Biology, Department of Oral Biology, Human Identification Research Center, Yonsei University College of Dentistry, Seoul, Korea

OPEN ACCESS

*Correspondence:
Ui-Won Jung
Department of Periodontology, Yonsei University College of Dentistry, 50 Yonsei-ro, Seodaemun-gu, Seoul 03722, Korea.
E-mail: drjew@yuhs.ac
Tel: +82-2-2228-3185
Fax: +82-2-392-0398

ORCID
Jin-Young Park
http://orcid.org/0000-0002-6408-1618
Jung-Ho Chung
http://orcid.org/0000-0003-4375-2213
Jung-Seok Lee
http://orcid.org/0000-0003-1276-5978
Hee-Jin Kim
http://orcid.org/0000-0002-1139-6261
Seong-Ho Choi
http://orcid.org/0000-0001-6704-6124
Ui-Won Jung
http://orcid.org/0000-0001-6371-4172

ABSTRACT

Purpose: Optical coherence tomography (OCT) is a noninvasive diagnostic technique that may be useful for both qualitative and quantitative analyses of the periodontium. Micro-computed tomography (micro-CT) is another noninvasive imaging technique capable of providing submicron spatial resolution. The purpose of this study was to present periodontal images obtained using *ex vivo* dental OCT and to compare OCT images with micro-CT images and histologic sections.

Methods: Images of *ex vivo* canine periodontal structures were obtained using OCT. Biologic depth measurements made using OCT were compared to measurements made on histologic sections prepared from the same sites. Visual comparisons were made among OCT, micro-CT, and histologic sections to evaluate whether anatomical details were accurately revealed by OCT.

Results: The periodontal tissue contour, gingival sulcus, and the presence of supragingival and subgingival calculus could be visualized using OCT. OCT was able to depict the surface topography of the dentogingival complex with higher resolution than micro-CT, but the imaging depth was typically limited to 1.2–1.5 mm. Biologic depth measurements made using OCT were a mean of 0.51 mm shallower than the histologic measurements.

Conclusions: Dental OCT as used in this study was able to generate high-resolution, cross-sectional images of the superficial portions of periodontal structures. Improvements in imaging depth and the development of an intraoral sensor are likely to make OCT a useful technique for periodontal applications.

Keywords: Diagnosis; Histology; Optical coherence tomography; Periodontal diseases

Generated by KAMJE PRESS

Author Contributions

Conceptualization: Ui-Won Jung; Data curation: Jin-Young Park; Formal analysis: Jin-Young Park; Funding acquisition: Ui-Won Jung; Investigation: Jin-Young Park; Methodology: Jin-Young Park, Ui-Won Jung; Project administration: Jin-Young Park, Ui-Won Jung; Resources: Jung-Ho Chung, Hee-Jin Kim; Software: Jung-Ho Chung; Supervision: Jung-Seok Lee, Seong-Ho Choi; Visualization: Jin-Young Park, Jung-Seok Lee; Writing - original draft: Jin-Young Park; Writing - review & editing: Ui-Won Jung, Jin-Young Park.

INTRODUCTION

Periodontitis is a prevalent disorder that affects most of the global population. Although a mild form of disease is compatible with good oral health, severe manifestations may lead to tooth loss [1]. The World Health Organization has reported that severe periodontitis is present in 5%–15% of people worldwide [2,3]. Furthermore, epidemiologic studies have shown that periodontal infection may also have implications for systemic health [3], suggesting that periodontitis is associated with a major oral health burden [4].

The periodontal diagnosis provides the clinician with information on the type, severity, and location of periodontal disease [5]. A periodontal examination is performed to detect clinical signs of pain and suppuration, the amount of observable plaque and calculus, probing depths (PDs), and the extent and pattern of loss of clinical attachment and bone. Traditional clinical investigation tools for routine periodontal examinations are periodontal probing and conventional radiography. In periodontal probing, a manual probe is placed between the soft tissue and tooth to evaluate the subgingival periodontal condition. The PD is measured as the depth of probe penetration from the gingival margin to the base of the crevice. However, periodontal probing is not only painful for the patient but also prone to diagnostic inaccuracy, primarily because it is performed without visual guidance. Errors in PD measurements may be caused by the presence of dental calculus and inconsistencies in the force of probe insertion, in the diameter of the probe tip, and in the anatomical tooth contours [6,7]. Moreover, reliable outcomes require the clinician to be sufficiently well trained in the technique.

The information provided by intraoral radiographs includes root length, root form, presence or absence of periapical lesions, dental calculus, root proximity, and remaining alveolar bone [5]. Conventional radiographs have a tendency to underestimate the amount of bone loss. Sequentially obtained radiographs have been shown to reveal bony changes that are detectable by the naked eye only after 30%–50% of the bone mineral has been absorbed [8,9]. This means that radiographs are not useful for identifying periodontal disease until after substantial bone loss has already occurred. On two-dimensional (2D) radiographs it is impossible to detect the precise location of a bony defect if the defect is located on the buccal or lingual side. Additionally, radiographs require exposure to harmful ionizing radiation and provide no information about the state of the soft tissues. Cone-beam computed tomography is routinely implemented in dentistry for imaging soft and hard tissues, especially for the diagnosis of oral pathology and three-dimensional (3D) analysis of orofacial structures. However, its common use for periodontal diagnosis cannot be justified due to its relatively low spatial resolution and the need to expose patients to relatively high levels of ionizing radiation. To the best of our knowledge, there is no device available for consistently quantifying or visualizing the oral soft tissues.

Optical coherence tomography (OCT) is a noninvasive diagnostic technique that detects mechanical interfaces based on differences in the reflection of light. OCT enables subsurface cross-sectional imaging with a resolution better than 10 times that of typical ultrasound imaging systems. OCT was initially developed for imaging the transparent tissues of the eye, but continuing advancements in OCT technology have led to the widespread use of existing prototypes in fields of gastroenterology, ophthalmology, dermatology, and dentistry. OCT could also be advantageous in dentistry, since this technology uses a nonionizing energy source, namely near-infrared light that cannot harm patients. In addition, several other

advantages, such as depth-resolved imaging, rapid acquisition of data, and the capability to observe both hard and soft tissues have made it attractive for many applications. OCT imaging of dental and periodontal microstructures may be useful for quantitative and qualitative assessments of oral tissues.

The aims of this study were; 1) to present periodontal images obtained using dental OCT, and 2) to compare OCT images with micro-computed tomography (micro-CT) images and histologic sections.

MATERIALS AND METHODS

Implementing *ex vivo* OCT

The OCT system (Prototype, LG Electronics, Seoul, Korea) developed for this study was based on the swept-source method (Figure 1). The swept source (AXP50124-8, Axsun Technologies, Boston, MA, USA) generates light at a center wavelength of 1,310 nm, with a repetition rate of 50 kHz, an average power of 10 mW, and a sweep range of 110 nm. The emitted beam is split in a directional coupler into 2 arms, reference and sample, with 90% of the beam passing through the sampler arm and 10% through the reference arm. The circulator in each arm directs these beams toward identical collimators. Then, in the sample arm, a 2D galvanometer system steers the beam and focuses it into the sample tissue via a scan lens. The scan lens has a numerical aperture of 0.026, resulting in a spot diameter of approximately 32 µm in air. Meanwhile, in the reference arm, the beam passes through a dispersion compensation block—to match the dispersion introduced by the scan lens—and is then reflected by a mirror. Both reflected beams are routed via the circulators toward another directional coupler, which evenly splits the 2 incoming beams into 2 ports. Each port transmitting the halves of the beam reflected from the sample and the reference
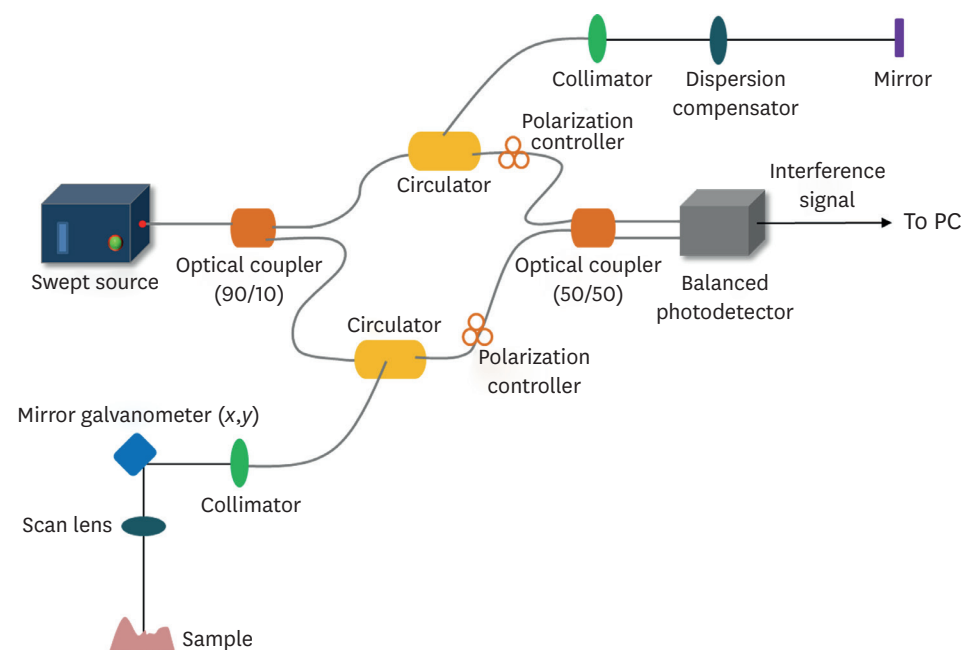
Figure 1. Schematic diagram of the prototype OCT system based on a swept source that generates light with a center wavelength of 1,310 nm.
OCT, optical coherence tomography.

mirror is connected to a balanced detector. This detector subtracts the signal from 1 port from that of the other to remove the common signal and leave only the interference signal. The polarization controllers in both arms are used to maximize the interference signal. The resulting signal is then processed on a PC to generate a depth-resolved intensity profile of the light backscattered from the tissue under investigation. This process is repeated whenever the galvanometer changes its angle in order to generate 2D or 3D images. The system has an imaging capability of capturing 25 frames per second with an axial resolution in air and water of 20 and 30 µm, respectively, and a lateral resolution of 32 µm. The 2D images present 500 pixels per column on the x-axis, corresponding to a maximum of 10 mm of scanning, and 512 pixels per column on the y-axis, corresponding to a maximum depth of 5 mm.

Preparation of tissue specimens

Animal selection and management, as well as the surgical protocol and preparation used in this study, followed protocols approved by the Institutional Animal Care and Use Committee, Yonsei Medical Center, Seoul, Korea (Permission No. 2011-0188). Five beagle dogs were used to produce the *ex vivo* specimens. Ten block-bone samples containing the second premolars from each side of the mandible were collected, and the specimens were preserved in 10% formalin prior to the experiments.

OCT imaging of *ex vivo* specimens

OCT images of the gingival sulcus and adjacent root surface were captured at the midbuccal aspect of the second mandibular premolars of the 10 specimens. A single blinded examiner measured the biologic depth in each captured image using the OCT software interface. The biologic depth was measured as the distance from the gingival margin to the base of the sulcus, as visible on each scanned image (Figure 2). In more detail, a combined vector (the biologic depth) was deduced from the horizontal and vertical measurements on the x- and y-axes of the OCT interface. The presence of dental calculus in the captured images was assessed based on the visible signal intensities.
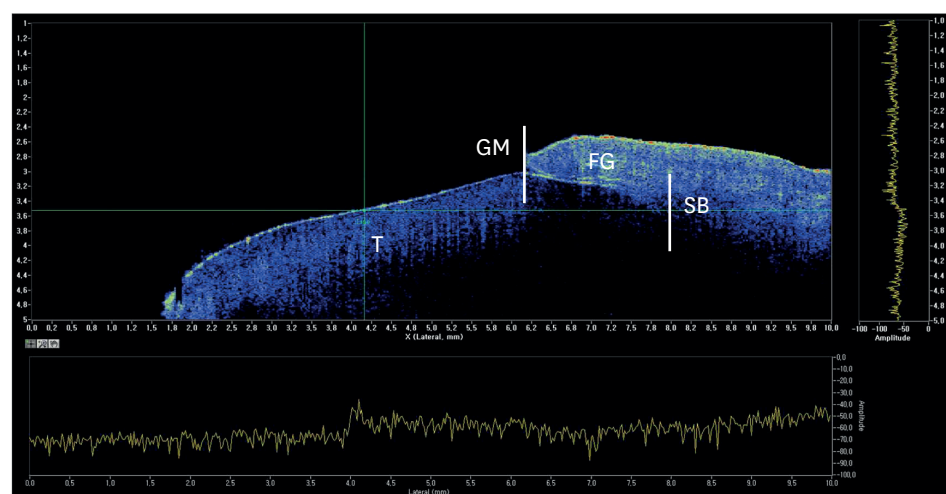
Figure 2. Captured image of the canine tooth model on the software interface of the *ex vivo* OCT system. The graphs represent the amplitude of light backscattered from the tissue; the x- and y-axes represent the scanning range and depth, respectively.

OCT, optical coherence tomography; T, tooth; GM, gingival margin; FG, free gingiva; SB, sulcus base.

Statistical analysis

Statistical analysis was performed with SPSS version 23 (IBM Corp., Armonk, NY, USA). To evaluate the measurement error, the intraclass correlation coefficient between the OCT and histologic measurements was calculated in a 2-way random model. In addition, the Bland-Altman method was used to evaluate the 2 techniques. In the Bland-Altman method, to determine whether there was a level of agreement between the 2 techniques or a proportional bias, the 1-sample t-test was used, followed by a visual inspection of the Bland-Altman plot, and then a linear regression analysis.

Micro-CT imaging of canine specimens

All harvested specimens were scanned with a micro-CT system (Sky-Scan 1173, SkyScan, Aartselaar, Belgium) at a resolution of 13.85 μm (achieved using 130 kV and 60 μA). The scanned data set was processed in Digital Imaging and Communications in Medicine (DICOM) format, and cross-sectional views and 3D images of the specimens were reconstructed with On-Demand 3D software (Cybermed, Seoul, Korea).

Histologic processing

Block sections of the surgical sites were fixed in 10% formalin for 10 days. The fixed specimens were decalcified in 5% formic acid for 14 days and then embedded in paraffin. Serial 5-μm-thick sections were cut buccolingually at the central portion of the second premolars. The midbuccal sections identical to the sites where measurements were made using OCT were selected and stained with hematoxylin and eosin for histologic observations. The histologic slides were observed and digitally captured under a light microscope (DM LB, Leica Microsystems, Wetzlar, Germany) equipped with a camera (BX50, Olympus, Tokyo, Japan). After examination using conventional microscopy, computer-assisted histometric measurements of periodontal dimensions, including the sulcus depth, gingival thickness, and epithelial and connective tissue thickness, were made using an automated image analysis system (Image-Pro Plus, Media Cybernetics, Silver Spring, MD, USA).

## RESULTS

Imaging of canine specimens using dental OCT

Periodontal anatomical structures were imaged using *ex vivo* dental OCT (Figure 2). The periodontal tissue contour, gingival sulcus, and the presence of supragingival and subgingival calculus could be visualized in high definition using the OCT system. The surface microstructural characteristics of both the tooth and gingiva could be assessed. The dentinoenamel junction (DEJ) could be seen in the tooth images. The deposition of dental calculus on tooth surfaces both above and below the gingival margin could be visualized, and this was confirmed in a graph produced using the software interface showing increased signal amplitude compared to the neighboring tooth surface (Figure 3). Calculus deposits or anomalous tooth surfaces presented as sharp peaks in signal amplitude compared to clean sites (Figure 4), and this finding was consistent in both supragingival and subgingival calculus specimens.

Depth measurements could be made using the software interface either in real time or on previously captured images. The epithelial layer and the subepithelial connective tissue layer were distinguishable in the images as different signal intensities (Figure 5A). The epithelial layer of the gingiva was measured at approximately 0.5 mm, which was consistent with the
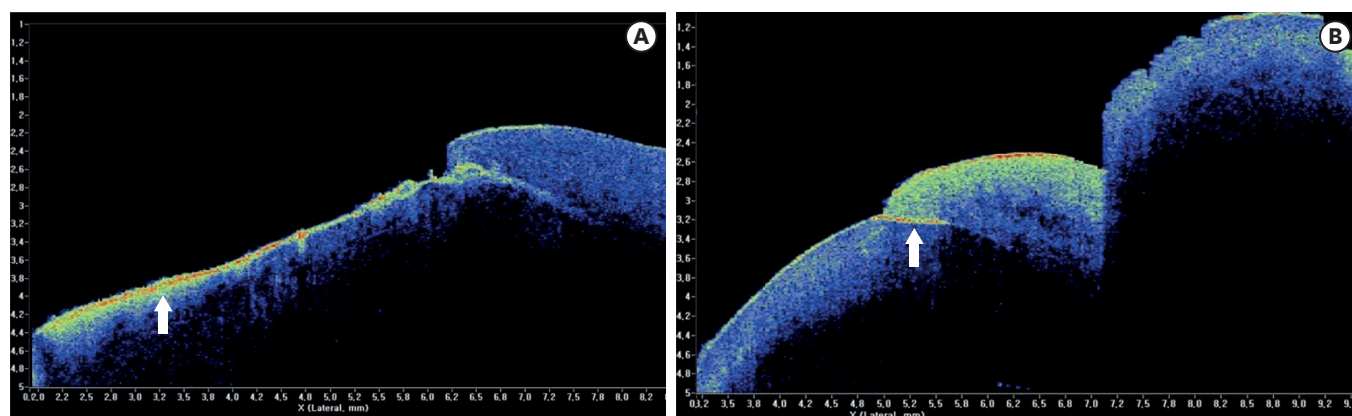
Figure 3. OCT imaging of the canine dentogingival complex. (A) Supragingival calculus (arrow) is clearly visualized on the tooth surface. (B) Subgingival calculus (arrow) can also be seen below the gingival margin with a signal intensity similar to that of supragingival calculus.

OCT, optical coherence tomography.
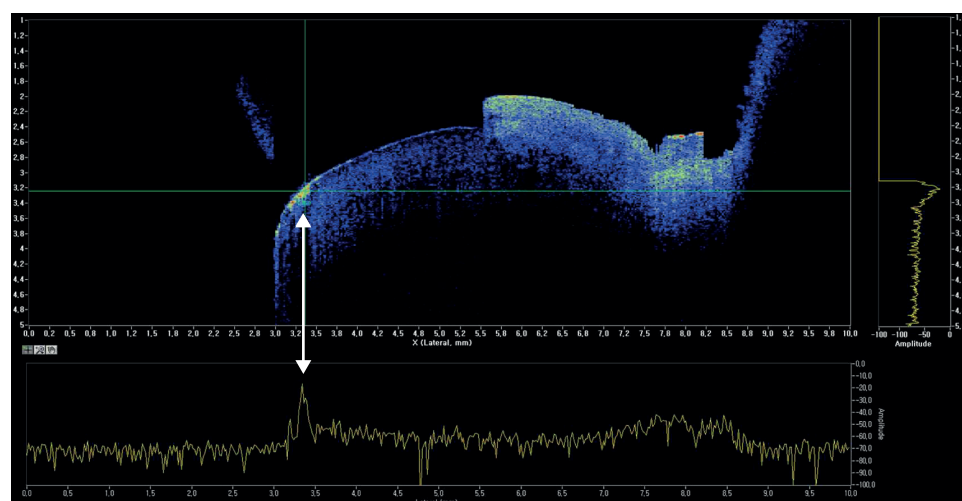
Figure 4. A tooth surface anomaly appears as increased signal intensity relative to adjacent surfaces, and is also evident in the amplitude graph (arrow).

histologic measurements. However, the overall imaging depth was typically 1.2–1.5 mm, which meant that the presence of alveolar bone could not be visualized on the images.

Comparison of biologic depth measurements between OCT and histology

The depth of the gingival sulcus as measured using OCT and histologically was compared (Table 1). This was performed at the midbuccal aspect of 10 mandibular second premolars. The OCT and histologic measurements showed an intraclass correlation coefficient of 0.220 (95% confidence interval: −2.141, 0.806), which suggests low correspondence between the two measurement methods. The Bland-Altman method revealed a significant level of disagreement between the 2 methods (P=0.008). Inspection of the Bland-Altman plot (Figure 6) showed that the differences in the measurements were greater at deeper biologic depths; however, statistically, no significant proportional bias was found (P=0.101). The mean difference between 2 methods for measurements at the 10 sites was 0.41 mm, with the OCT measurements being shallower (1.20±0.19 mm) than the histologic measurements (1.61±0.35 mm).
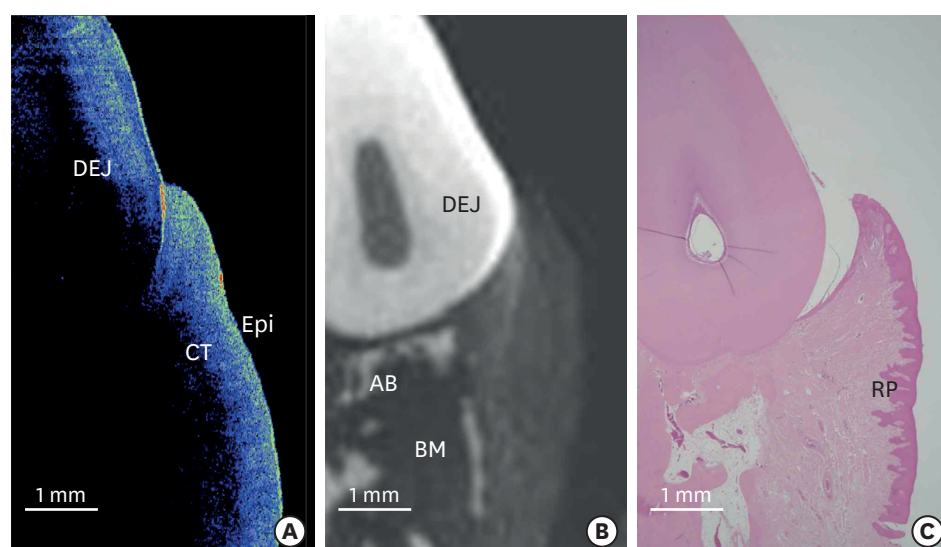
Figure 5. Comparison of (A) OCT, (B) micro-CT, and (C) histology at the buccal furcation region of the second premolar of a canine specimen. The surface topography is more accurately revealed by OCT than by micro-CT. (A) The epithelial thickness appears as a brighter green coloration at the superficial surface of the gingiva, in comparison to the darker blue area corresponding to the loose connective tissue directly underneath. (B) Visualization of gingival soft tissue in a micro-CT image, but with less visual acuity than in the OCT image. Alveolar bone including the bone marrow space can be observed. (C) Histologic section showing the rete pegs of the epithelium lining the gingiva with adjacent loose connective tissue. Alveolar bone can be seen below the furcation with its marrow space. (H&E, ×10).

OCT, optical coherence tomography; micro-CT, micro-computed tomography; H&E, hematoxylin and eosin; DEJ, dentinoenamel junction; CT, connective tissue; Epi, epithelium; AB, alveolar bone; BM, bone marrow; RP, rete pegs.

Table 1. Biologic depth measurements using OCT and histology performed on the midbuccal aspect of 10 *ex vivo* second mandibular premolars of dogs

| Sample	1	2	3	4	5	6	7	8	9	10	Mean	SD
OCT (mm)	0.94	1.30	1.12	1.39	1.21	1.49	0.94	1.39	1.21	1.03	1.20	0.19
Histology (mm)	1.38	1.48	1.92	1.12	1.19	2.20	1.53	1.54	2.04	1.68	1.61	0.35

OCT, optical coherence tomography; SD, standard deviation.
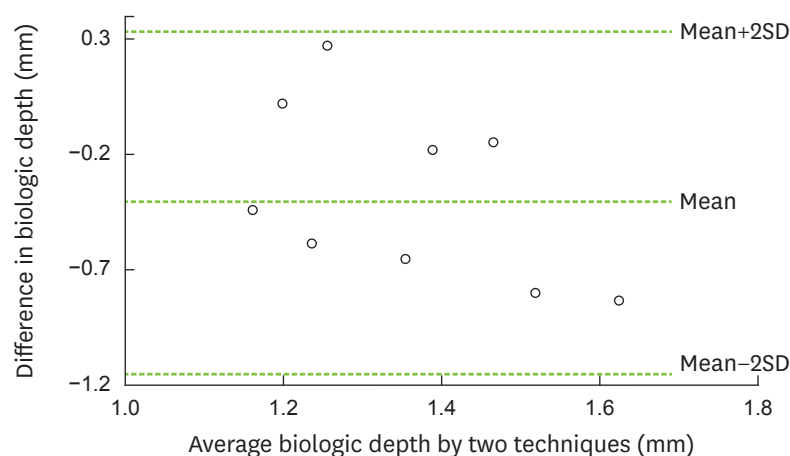
Figure 6. A Bland-Altman plot showing the differences in biologic depth measurements between OCT and histology. OCT, optical coherence tomography; SD, standard deviation.

Micro-CT representation of canine specimens

The micro-CT images could effectively display the teeth and surrounding alveolar bone in 3D reconstruction views as well as in cross-sectional views (Figure 7). In the cross-sectional view,
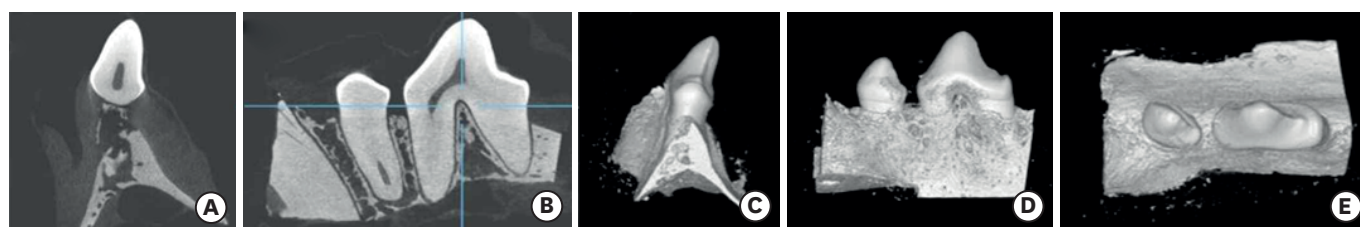
Figure 7. Micro-CT images of the canine dentogingival complex in the (A) coronal and (B) sagittal planes. Three-dimensional reconstructed images are shown in the (C) distal, (D) buccal, and (E) occlusal planes.
Micro-CT, micro-computed tomography.

the dense cortical outline of the alveolar bone could be seen, bundle bone surrounded the roots of the teeth, and cancellous bone with an interconnected trabecular pattern was evident in detail against the radiolucent bone marrow (Figure 7B) [10]. The internal structures of the teeth could also be observed; the presence of the DEJ was clearly depicted due to the high radiopacity of the enamel. Such details were not visible on OCT images due to the poor imaging penetration.

Soft-tissue contours could be made visible by appropriately adjusting the grayscale used to display the images. The gingival outline including the location of the vestibule could be seen, and the thickness of the soft tissue could be measured from the bone in cross-sectional views. However, certain aspects of the microstructural architecture, such as the gingival sulcus and connective tissue attachments, could not be distinguished.

Histologic representation of canine specimens

Histologic sections were used as the gold standard in comparisons with OCT and micro-CT images (Figure 5C). The process of embedding paraffin wax into the gingival sulcus had expanded the space inside the sulcus, and so the histologic sections appeared different from the *ex vivo* OCT images. However, the overall shape of the tooth and the surrounding soft-tissue contours remained very similar. The DEJ was evident only in some sections, and in those, the enamel appeared to be thinner. This may have been caused by the dissolution of enamel during the decalcification process using formic acid. Orthokeratinized gingival epithelium formed long rete pegs against the underlying connective tissue, unlike the junctional epithelium, which appeared to be only a few cells thick, flat, and without rete pegs (Figure 5C). The histologic slides were obtained from the coronal section of the furcation area. The furcation was chosen deliberately since it is frequently associated with the progression of periodontal disease. However, despite the natural accumulation of calculus at some sites, no significant attachment loss resulting in furcation involvement was detected.

DISCUSSION

The findings of this study indicate that OCT can be used as a noninvasive method for imaging the dental microstructure. The current OCT prototype system operates in the Fourier domain (FD). One advantage of FD-OCT over previous OCT systems is that it simultaneously provides high-speed and wide-field imaging. Depending on the method of illumination, FD-OCT can be classified into spectral-domain OCT and swept-source OCT (SS-OCT). This study used an SS-OCT prototype for imaging the periodontal tissues, and assessed its accuracy in periodontal diagnosis.

Determining the accuracy of measurements of the sulcular depth using the current OCT interface was one of the main objectives of this study, in order to ascertain the feasibility of using it in clinical applications. The biologic depth measurements made using OCT images were a mean of 0.41 mm shallower than those made in the histologic sections, which were considered the gold standard. The measurements were carried out in the buccal furcation area of the mandibular premolars; this area was deliberately chosen since it is frequently affected by periodontitis. The imaging depth required to observe the gingival attachment is greater inside the furcation than in other areas, due to the horizontal component of the furcal concavity. The cross-sectional imaging depth of the OCT system used in this study was found to be insufficient for visualizing the sulcus anatomy within the furcation, which is probably the main reason for the discrepancy between the depth measurements made using OCT and histologically.

The imaging depth of OCT is an important aspect of the imaging quality, and it is determined by 2 main factors: the wavelength of the light source and the numerical aperture of the light-collecting optics [11]. Otis et al. [11] showed that the image quality could be improved by increasing the imaging depth, and that the penetration depth could be increased by increasing the center wavelength of the light source. Similar results were obtained in a recent study of the porcine jaw, in which the performance of SS-OCT at 1,325 nm was better than that at 930 nm owing to the longer center wavelength that allowed deeper tissue penetration [12]. In a highly scattering media such as biologic tissue, the intensity of coherent backscattered light decays exponentially with depth. Moreover, increasing the source intensity has only a small effect on the imaging depth of OCT since the scattering coefficient is independent of the source power [13]. In contrast, increasing the wavelength significantly reduces the scattering coefficient for many biologic tissues, including enamel and gingiva, but potentially decreases the spatial resolution of OCT images. A larger numerical aperture also improves the imaging depth resolution, since the reflected light is collected over a larger range of scattering angles. The OCT system used in the present study had a relatively long center wavelength of 1,310 nm with a numerical aperture of 0.026. Further developments in dental OCT are needed to improve both the imaging depth and the imaging quality before it can be utilized in periodontal applications.

The periodontal tissue contour, dental calculus, and connective tissue attachment were visualized in high definition using OCT in this study. Such detailed visualization of biologic tissues could be very useful in several fields of dentistry. This may allow the early detection of active periodontal disease or causative factors such as subgingival calculus, before significant alveolar bone loss occurs. The captured images could be stored as a permanent record for comparison with future periodontal examinations in order to detect changes in PDs or the inflammatory response at sites of interest. This would provide valuable information during both the diagnostic and maintenance phases of periodontal therapy for the detection of disease recurrence or sites where periodontal treatment has been ineffective.

The current software interface allows the measurement of gingival thickness, which is a predictor of the gingival phenotype. *In vivo* visualization of the oral mucosa at the microscopic level has been documented previously [14]. Although the image sharpness is affected by the axial resolution and signal-to-noise ratio, it is possible to vaguely discriminate between the epithelium and subepithelial connective tissue. Such information can be immensely valuable and have implications for the results of periodontal therapy, gingival augmentation procedures, root coverage, and implants in esthetic areas where the adequacy of the gingival thickness is paramount. Determining the thickness of the epithelial layer can be especially

useful during the planning and execution of connective tissue grafting procedures, since this could confirm the sufficiency of undermining of the epithelium at the graft site. Furthermore, bleeding at the donor site could be reduced if palatal vessels are visualized. Several methods for evaluating gingival thickness, such as injection needles, probe transparency, and visual inspection, cannot be considered reliable due to their subjective nature. The main advantage of OCT over these techniques is that it is a quantitative high-resolution imaging method that can be used in real time during clinical procedures.

Brezinski et al. [15] showed that the contrast between different adjacent tissue types is stronger when there is a greater difference in the water content within tissues. Similarly, in the present study, the samples that included subgingival calculus would have had higher water content than the adjacent tooth surface, resulting in an increased signal intensity and contrast. We may assume that the presence of gingival crevicular fluid in an *in vivo* model would allow better visualization of the sulcular anatomy compared to the *ex vivo* model. We could therefore expect a greater penetration depth in humans than in the dogs used in this study since the density of gingival tissues is likely to be lower in humans. Furthermore, greater transparency and signal amplitudes can be anticipated in pathologic areas characterized by swelling of gingiva. Future studies involving humans should investigate different gingival biotypes or pathologic tissues in order to test the clinical performance of dental OCT.

A limitation of this study was the small sample size. Sulcus depth measurements were made at only 10 sites, which resulted in a low statistical power. The number of samples was restricted by the need to sacrifice animals for such *ex vivo* examinations. Coupling the instrument to an intraoral sensor would permit the acquisition of more relevant and robust information in future studies.

The method of dental OCT investigated in this study was able to generate high-resolution cross-sectional images of the superficial portions of the periodontal structures. Future improvements in imaging depth and the development of an intraoral sensor are likely to make OCT a useful technique for periodontal applications.

ACKNOWLEDGEMENTS

REFERENCES

1. Brown LJ, Löe H. Prevalence, extent, severity and progression of periodontal disease. Periodontol 2000 1993;2:57-71.
   PUBMED | CROSSREF
2. Petersen PE. The World Oral Health Report 2003: continuous improvement of oral health in the 21st century--the approach of the WHO Global Oral Health Programme. Community Dent Oral Epidemiol 2003;31 Suppl 1:3-23.
   PUBMED | CROSSREF

3. Burt BResearch, Science and Therapy Committee of the American Academy of Periodontology. Position paper: epidemiology of periodontal diseases. J Periodontol 2005;76:1406-19.
   PUBMED | CROSSREF

4. Petersen PE, Ogawa H. The global burden of periodontal disease: towards integration with chronic disease prevention and control. Periodontol 2000 2012;60:15-39.
   PUBMED | CROSSREF

5. Armitage GCResearch, Science and Therapy Committee of the American Academy of Periodontology. Diagnosis of periodontal diseases. J Periodontol 2003;74:1237-47.
   PUBMED | CROSSREF

6. Pihlstrom BL. Measurement of attachment level in clinical trials: probing methods. J Periodontol 1992;63:1072-7.
   PUBMED | CROSSREF

7. Mayfield L, Bratthall G, Attström R. Periodontal probe precision using 4 different periodontal probes. J Clin Periodontol 1996;23:76-82.
   PUBMED | CROSSREF

8. Molander B, Ahlqwist M, Gröndahl HG, Hollender L. Comparison of panoramic and intraoral radiography for the diagnosis of caries and periapical pathology. Dentomaxillofac Radiol 1993;22:28-32.
   PUBMED | CROSSREF

9. Jeffcoat MK, Wang IC, Reddy MS. Radiographic diagnosis in periodontics. Periodontol 2000 1995;7:54-68.
   PUBMED | CROSSREF

10. Croucher PI, Garrahan NJ, Compston JE. Assessment of cancellous bone structure: comparison of strut analysis, trabecular bone pattern factor, and marrow space star volume. J Bone Miner Res 1996;11:955-61.
    PUBMED | CROSSREF

11. Otis LL, Colston BW Jr, Everett MJ, Nathel H. Dental optical coherence tomography: a comparison of two *in vitro* systems. Dentomaxillofac Radiol 2000;29:85-9.
    PUBMED | CROSSREF

12. Mota CC, Fernandes LO, Cimões R, Gomes AS. Non-invasive periodontal probing through fourier-domain optical coherence tomography. J Periodontol 2015;86:1087-94.
    PUBMED | CROSSREF

13. Fried D, Glena RE, Featherstone JD, Seka W. Nature of light scattering in dental enamel and dentin at visible and near-infrared wavelengths. Appl Opt 1995;34:1278-85.
    PUBMED | CROSSREF

14. Feldchtein F, Gelikonov V, Iksanov R, Gelikonov G, Kuranov R, Sergeev A, et al. *In vivo* OCT imaging of hard and soft tissue of the oral cavity. Opt Express 1998;3:239-50.
    PUBMED | CROSSREF

15. Brezinski ME, Tearney GJ, Bouma BE, Izatt JA, Hee MR, Swanson EA, et al. Optical coherence tomography for optical biopsy. Properties and demonstration of vascular pathology. Circulation 1996;93:1206-13.
    PUBMED | CROSSREF